

Leptoquark Pair Production at ep Colliders

Johannes Blümlein¹, Edward Boos^{1,2}, and Alexander Pukhov²

¹*DESY – Institut für Hochenergiephysik Zeuthen,
Platanenallee 6, D-15735 Zeuthen, Germany*

²*Institute of Nuclear Physics, Moscow State University,
RU-119899 Moscow, Russia*

Abstract

The pair production cross section for scalar and vector leptoquarks at ep colliders is calculated for the case of photon-gluon fusion. In a model independent analysis we consider the most general C and P conserving couplings of gluons and photons to both scalar and vector leptoquarks described by an effective low-energy Lagrangian which obeys $U(1)_{em} \times SU(3)_c$ invariance. Numerical predictions are given for the kinematical regime at HERA and LEP \otimes LHC.

hep-ph/9404321 20 Apr 1994

1 Introduction

Many theories beyond the Standard Model try to unify the observed quark and lepton degrees of freedom on a more fundamental level [1]. As a consequence, new bosons, the leptoquarks, are contained in these models. For a long time ep colliders have been considered as ideal facilities to search for leptoquarks through $e^\pm q(\bar{q})$ fusion [2, 3], since their signal emerges as a narrow peak in the deep inelastic differential $e^\pm p$ scattering cross sections $d^2\sigma^{e^\pm p}/dx dQ^2$. Searching for these peaks, the first experimental limits from collider experiments on the mass and the $l^\pm q(\bar{q})$ couplings, λ_{lq} , of leptoquarks to the fermions of the first generation have been given by ZEUS and H1 (cf. [4]) at HERA recently. The couplings λ_{lq} are *not* predicted by theory and it is not excluded that $\lambda_{lq}/e \ll 1$. In fact, a recent re-analysis of different measurements with respect to leptoquark contributions [5] constrains $\lambda_{lq}/e \lesssim 0.07\dots 0.27$, depending on the type of scalar and vector leptoquarks. For $\lambda_{lq}/e \ll 1$ both the production cross sections for $e^\pm q(\bar{q})$ fusion and $e^\pm g$ fusion [6] are rather small.

Leptoquark pair production via photon-gluon fusion depends on the gauge boson couplings to leptoquarks *only*. Thus, a dedicated search for leptoquarks is possible also in the range of small fermion couplings. In the case of scalar leptoquarks all couplings are known completely ¹. For vector leptoquarks the situation is more complex and depends on the specific nature of the low-energy leptoquark states emerging after symmetry breaking in a unified theory or in some scenario of compositeness. To keep the analysis as model independent as possible we assume the most general Lorentz structure for photon and gluon-leptoquark couplings which respect C and P conservation [8]. The cases of a minimal vector boson coupling (cf. [9]) and a Yang-Mills type coupling are contained in this description as well as the 'anomalous' couplings $\kappa_{A,G}$ and $\lambda_{A,G}$. These parameters determine the production cross sections in addition to the known electromagnetic and color couplings.

In this letter we derive the pair production cross sections for vector leptoquarks based on photon-gluon fusion (section 2). The expectations to produce the different types of scalar and vector leptoquarks at HERA and possible future experiments at LEP \times LHC are discussed in section 3. An appendix summarizes the functions which describe the differential and integrated cross section of vector leptoquark pair production.

2 Production Cross Sections

We will calculate the contributions to leptoquark pair production due to photon-gluon fusion and consider the direct terms only. The resolved photon contributions are dealt with in a separate paper [10] ². The Feynman diagrams which determine both the scalar and vector leptoquark pair production cross sections are shown in figure 1. Note, that contrary to the case of e^+e^- annihilation [9] Yukawa-type fermion couplings do not contribute. The interaction of the different leptoquarks species with photons and gluons is described by the effective Lagrangian in equ. (1) which is constructed to be invariant under $U(1)_{em} \times SU(3)_c$ gauge transformations.

$$\mathcal{L} = \mathcal{L}_s + \mathcal{L}_v \quad (1)$$

¹The structure of the scattering cross section for this case has been known from scalar electrodynamics for a very long time [7]. We include a brief discussion of scalars only for the purpose of a systematic comparison with respect to the classification of leptoquark states [3] and as a numerical update.

²At high virtualities, Q^2 , of the intermediate boson terms due to γ - Z interference and Z -exchange also become relevant. Furthermore, pairs of different type leptoquarks (cf. [9]) can be produced via $W^\pm g$ fusion in this kinematical range.

with

$$\mathcal{L}_s = \sum_{\text{scalar } s} \left[(D^\mu \Phi)^\dagger (D_\mu \Phi) - M_s^2 \Phi^\dagger \Phi \right] \quad (2)$$

and ³

$$\begin{aligned} \mathcal{L}_v = & \sum_{\text{vectors}} \left\{ -\frac{1}{2} G_{\mu\nu}^\dagger G^{\mu\nu} + M_v^2 \Phi_\mu^\dagger \Phi^\mu - ie \left[(1 - \kappa_A) \Phi_\mu^\dagger \Phi_\nu F^{\mu\nu} + \frac{\lambda_A}{M_v^2} G_{\sigma\mu}^\dagger G_\nu^\mu F^{\nu\sigma} \right] \right. \\ & \left. - ig_s \left[(1 - \kappa_G) \Phi_\mu^\dagger \frac{\lambda^a}{2} \Phi_\nu G_a^{\mu\nu} + \frac{\lambda_G}{M_v^2} G_{\sigma\mu}^\dagger \frac{\lambda^a}{2} G_\nu^\mu G_a^{\nu\sigma} \right] \right\}. \end{aligned} \quad (3)$$

Here e and g_s denote the electromagnetic and strong coupling constant, and $\kappa_{A,G}$ and $\lambda_{A,G}$ are the anomalous couplings. The field strength tensors of the photon-, gluon-, and vector leptoquark fields are

$$\begin{aligned} F_{\mu\nu} &= \partial_\mu A_\nu - \partial_\nu A_\mu, \\ \mathcal{G}_{\mu\nu}^a &= \partial_\mu \mathcal{A}_\nu^a - \partial_\nu \mathcal{A}_\mu^a + if^{abc} \mathcal{A}_{\mu b} \mathcal{A}_{\nu c}, \\ G_{\mu\nu} &= D_\mu \Phi_\nu - D_\nu \Phi_\mu \end{aligned} \quad (4)$$

with the covariant derivative given as

$$D_\mu = \partial_\mu - ieQ^\gamma A_\mu - ig_s \frac{\lambda^a}{2} \mathcal{A}_\mu^a. \quad (5)$$

The parameters $\kappa_{A,G}$ and $\lambda_{A,G}$ are assumed to be real. They are related to the anomalous 'magnetic' moment μ_Φ and 'electric' quadrupole moment q_Φ of the leptoquarks in the electromagnetic and color fields

$$\begin{aligned} \mu_{\Phi,\alpha} &= \frac{g_\alpha}{2M_\Phi} (2 - \kappa_\alpha + \lambda_\alpha) \\ q_{\Phi,\alpha} &= -\frac{g_\alpha}{M_\Phi^2} (1 - \kappa_\alpha - \lambda_\alpha) \end{aligned} \quad (6)$$

where $g_\alpha = e$ or g_s and $\alpha = A$ or G ⁴.

In particular we assume that these quantities are all independent since we wish to keep the analysis as model independent as possible.

We consider the leptoquarks which have been classified in [3, 9]. They are color triplets or anti-triplets, and the magnitude of their electric charges $|Q_\Phi|$ can take the values 5/3, 4/3, 2/3, or 1/3. The cross sections are calculated using the (improved) Weizsäcker–Williams approximation (WWA) [12].

The integrated pair production cross sections read

$$\sigma_{s,v}(S, M_\Phi^2) = \int_{y_{min}}^{y_{max}} dy \int_{x_{min}}^{x_{max}} dx \int_{-1}^1 d \cos \theta \phi_{\gamma/e}(y) G_{g/p}(x, \mu^2) \frac{d\hat{\sigma}_{s,v}}{d \cos \theta} \theta(\hat{s} - 4M_\Phi^2). \quad (7)$$

Here $d\hat{\sigma}_{s,v}/d \cos \theta$ denotes the differential cross section in the photon–gluon center-of-momentum system (cms), $G_{g/p}(x, \mu^2)$ is the gluon distribution at the factorization mass μ , $S = 4E_e E_p$,

³In compositeness scenarios one might wish to relate the quantities $\kappa_{A,G}$ and $\lambda_{A,G}$ to the compositeness scale Λ . This can be achieved e.g. rescaling these quantities by factor M_v^2/Λ^2 .

⁴Note that the convention for the κ_A and λ_A used here translates into that of [11] by substituting $\kappa_A = 1 - \kappa_\gamma$, $\lambda_A = \lambda_\gamma$.

$\hat{s} = xyS$, x is the longitudinal momentum fraction of the proton carried by the gluon, and M_Φ denotes the mass of the leptoquarks. The photon distribution is described in WWA by

$$\phi_{\gamma/e}(y) = \frac{\alpha}{2\pi} \left[2m_e^2 y \left(\frac{1}{Q_{max}^2} - \frac{1}{Q_{min}^2} \right) + \frac{1 + (1-y)^2}{y} \log \frac{Q_{max}^2}{Q_{min}^2} \right]. \quad (8)$$

The kinematical boundaries in (7) and (8) are:

$$\begin{aligned} Q_{min}^2 &= \frac{m_e^2 y^2}{1-y} & Q_{max}^2 &= yS - 4M_\Phi^2 - 4M_\Phi m_p \\ x_{min} &= \frac{4M_\Phi^2}{yS} & x_{max} &= 1 \\ y_{min,max} &= \frac{S + \widetilde{W}^2 \pm \sqrt{(S - \widetilde{W}^2)^2 - 4m_e^2 \widetilde{W}^2}}{2(S + m_e^2)} \end{aligned} \quad (9)$$

where $\widetilde{W}^2 = (2M_\Phi + m_p)^2 - m_p^2$, m_e and m_p are the electron and proton mass, respectively, $y = P.q/P.l_e$, with $q = l_e - l'_e$, and P, l_e, l'_e the four momenta of the proton, the incoming and outgoing electron.

2.1 Scalar Leptoquarks

The differential and integrated production cross sections in the γ - g cms are⁵

$$\frac{d\hat{\sigma}_s}{d \cos \theta} = \frac{\pi \alpha \alpha_s(\mu^2)}{2\hat{s}} Q_\Phi^2 \beta \left\{ 1 - \frac{2(1-\beta^2)}{1-\beta^2 \cos^2 \theta} + \frac{2(1-\beta^2)^2}{(1-\beta^2 \cos^2 \theta)^2} \right\} \quad (10)$$

and

$$\hat{\sigma}_s(\hat{s}, \beta) = \frac{\pi \alpha \alpha_s(\mu^2)}{2\hat{s}} Q_\Phi^2 \left\{ 2(2-\beta^2)\beta - (1-\beta^4) \log \left| \frac{1+\beta}{1-\beta} \right| \right\}. \quad (11)$$

Here, $\beta = \sqrt{1 - 4M_\Phi^2/\hat{s}}$ and α_s denotes the strong coupling constant. The production cross section varies $\propto Q_\Phi^2$. For the leptoquark states classified in [3] one obtains e.g. $\sigma_s(R_2^{5/3}) = 25 \sigma_s(S_3^{1/3})$, etc.⁶

2.2 Vector Leptoquarks

The corresponding cross sections for vector leptoquarks can be represented in terms of the individual $A \leftrightarrow G$ symmetric combinations of $\kappa_{A,G}$ and $\lambda_{A,G}$ at tree level. The differential cross section in the γ - g cms is

$$\frac{d\hat{\sigma}_v}{d \cos \theta} = \frac{\pi \alpha \alpha_s(\mu^2)}{2\hat{s}} Q_\Phi^2 \sum_{j=0}^{20} \chi_j(\kappa_{A,G}, \lambda_{A,G}) \frac{F_j(\hat{s}, \beta, \cos \theta)}{(1-\beta^2 \cos^2 \theta)^2} \quad (12)$$

⁵The form of the cross section (10,11) has been derived in [7] and was used mutually in the literature for various processes [13] with different couplings and group theoretical factors.

⁶In the case of leptoquark pair production through $\gamma\gamma$ fusion [14], the ratio of the production cross sections varies even by factors up to 625.

with

$$\begin{aligned}
\sum_{j=0}^{20} \chi_j(\kappa_{A,G}, \lambda_{A,G}) F_j &= F_0 + (\kappa_A + \kappa_G) F_1 \\
&+ (\kappa_A^2 + \kappa_G^2) F_2 + \kappa_A \kappa_G F_3 \\
&+ \kappa_A \kappa_G (\kappa_A + \kappa_G) F_4 + \kappa_A^2 \kappa_G^2 F_5 \\
&+ (\lambda_A + \lambda_G) F_6 + (\lambda_A^2 + \lambda_G^2) F_7 \\
&+ \lambda_A \lambda_G F_8 + \lambda_A \lambda_G (\lambda_A + \lambda_G) F_9 \\
&+ \lambda_A^2 \lambda_G^2 F_{10} + (\kappa_A \lambda_A + \kappa_G \lambda_G) F_{11} \\
&+ (\kappa_A \lambda_G + \kappa_G \lambda_A) F_{12} + \lambda_A \lambda_G (\kappa_A + \kappa_G) F_{13} \\
&+ (\kappa_A \lambda_G^2 + \kappa_G \lambda_A^2) F_{14} + \lambda_A \lambda_G (\kappa_A \lambda_G + \kappa_G \lambda_A) F_{15} \\
&+ (\kappa_A^2 \lambda_G + \kappa_G^2 \lambda_A) F_{16} + (\kappa_A^2 \lambda_G^2 + \kappa_G^2 \lambda_A^2) F_{17} \\
&+ \kappa_A \kappa_G (\lambda_A + \lambda_G) F_{18} + \kappa_A \kappa_G \lambda_A \lambda_G F_{19} \\
&+ \kappa_A \kappa_G (\kappa_A \lambda_G + \kappa_G \lambda_A) F_{20}
\end{aligned}$$

and the integrated cross section reads

$$\hat{\sigma}_v = \frac{\pi \alpha \alpha_s (\mu^2)}{M_v^2} Q_\Phi^2 \sum_{j=0}^{20} \chi_j(\kappa_{A,G}, \lambda_{A,G}) \tilde{F}_j(\hat{s}, \beta) \quad (13)$$

where

$$\tilde{F}_j = \frac{M_v^2}{\hat{s}} \int_0^\beta d\xi \frac{F_j(\xi = \beta \cos \theta)}{(1 - \xi^2)^2}. \quad (14)$$

The functions $F_j(\hat{s}, \beta, \cos \theta)$ and $\tilde{F}_j(\hat{s}, \beta)$ are obtained in a lengthy but straightforward calculation which has been performed using the package CompHEP [15]. They are given in eqs. (17,18) in the appendix.

For the case $\kappa_A = \kappa_G$ and $\lambda_A = \lambda_G$ the equations (17) agree with results obtained in [11] for the case of W -boson pair production in γ - γ fusion. Other more specific results derived earlier for particular choices of κ and λ [16] are described by (12). In our notation the case $\kappa_{A,G} = \lambda_{A,G} \equiv 0$ corresponds to Yang-Mills type couplings of photons and gluons to vector leptoquarks, while $\kappa_{A,G} = 1, \lambda_{A,G} = 0$ describes the case of 'minimal' vector boson couplings [17]. Most of the above terms contain contributions $\propto (\hat{s}/M_\Phi^2)^n$ which are of $\mathcal{O}(1)$ in the threshold range. These unitarity-violating terms (for $\hat{s} \gg M_v^2$) are absent in some of the functions \tilde{F}_j , particularly for the contributions which are at most *linear* in $\kappa_{A,G}$ and $\lambda_{A,G}$.

One may ask whether apart from the Yang-Mills case another combination of these couplings exists which preserves tree-level unitarity. Since only in \tilde{F}_{10} a term $\propto (\hat{s}/M_\Phi^2)^3$ appears either λ_A or λ_G must vanish to preserve unitarity. Furthermore, the terms $\propto (\hat{s}/M_\Phi^2)^2$ cancel only for

$$\lambda_{A(G)}^2 [1 + (1 - \kappa_{G(A)}^2)^2] = 0 \quad (15)$$

Both λ_A and λ_G have to vanish to obtain real solutions. The terms $\propto (\hat{s}/M_\Phi^2)$ cancel if κ_A and κ_G obey the relation

$$(\kappa_A + \kappa_G - \kappa_A \kappa_G)^2 + \frac{2}{3} \kappa_A^2 \kappa_G^2 = 0. \quad (16)$$

Thus, for any non vanishing values of $\kappa_A, \kappa_G, \lambda_A, \lambda_G$ tree-level unitarity is not preserved by σ_v . At high energies (i.e. $\hat{s} \gg 4M_v^2$) the effective low energy Lagrangian (1) is no longer valid since terms which decouple at low energies become relevant. Instead one has to consider the full gauge theory from which (1) was obtained.

3 Numerical Results

In the subsequent numerical calculations we used the CTEQ2 (LO) parametrization to describe the gluon distribution [18]. Other recent parametrizations [19] yield similar numerical results. The factorization mass μ and the scale of α_s were chosen to be $\sqrt{\hat{s}}$. The uncertainty of the cross section calculation due to the use of the improved Weizsäcker–Williams approximation [12] was estimated to be of $\mathcal{O}(6\%)$ both for the case of HERA and LEP \times LHC due to the choice of the kinematical bounds (9a).

In figure 2a the integrated cross section for ep scattering at HERA is shown for scalar leptoquarks with $|Q_\Phi| = 1/3$ and $5/3$, respectively. Production cross sections $\sigma_s^{tot} \gtrsim 0.1pb$ – corresponding to 10 events at an integrated luminosity of $\mathcal{L} = 100pb^{-1}$ – are obtained for the states with $|Q_\Phi| = 2/3$ to $|Q_\Phi| = 5/3$ for $M_\Phi < 55$ to 65 GeV. For $|Q_\Phi| = 1/3$ the production cross section is too small for $M_\Phi \gtrsim 45$ GeV, a bound set previously by the LEP experiments [20]. At LEP \times LHC the search limits on a rate of 10 events extend from $M_\Phi = 140$ GeV for $|Q_\Phi| = 1/3$ to $M_\Phi = 220$ GeV for $|Q_\Phi| = 5/3$ assuming $\mathcal{L} = 1fb^{-1}$ as shown in figure 2b.

Limits on the allowed mass range of scalar leptoquarks have been derived by different experiments. Bounds which are independent of the leptoquark–fermion couplings were given by the LEP experiments as $M_\Phi > 44.4$ GeV at 95 % CL [20, 21]⁷ for almost all scalars classified in [3] and all three generations. Other limits have been found by the UA2 [23], CDF and D0 [24] experiments for the 1st generation scalar leptoquarks, excluding the mass ranges between 44 and 132 GeV depending on the branching ratios $Br(\Phi_s \rightarrow eq)$. Independently of the yet unknown fermion couplings $\lambda_{L,R}$, the states $\tilde{S}_1, S_3^{4/3}, R_2^{5/3}$ and $\tilde{R}_2^{2/3}$ are excluded for masses $M_\Phi < 132$ GeV and the state S_1 for $M_\Phi < 86$ GeV. For general values of the fermion couplings, the states $S_3^{-2/3}, \tilde{R}_2^{-1/3}, R_2^{2/3}$ and $S_3^{1/3}$ are constrained by the LEP bound only. Unlike these partial results a systematic search for scalar leptoquarks of *all* generations above the LEP limit is still needed in the kinematically accessible range at HERA, $M_\Phi \lesssim 63$ GeV. Among the different states [3] the search for $S_3^{-2/3}$ and $\tilde{R}_2^{2/3}$ (with $\lambda_R = 0$) (cf. [9]) is particularly difficult, since these leptoquarks decay only into a neutrino–quark pair, a signature with a large QCD background.

Figure 3a shows the integrated cross section for vector leptoquark pair production at HERA for different choices of $\kappa_{A,G}$ and $\lambda_{A,G}$. In a model independent analysis the complete dependences on these four parameters must be explored. From the examples shown in figure 3a it is evident, that severe constraints on the parameter space of the anomalous couplings can be obtained at HERA. Complementary to searches at $p\bar{p}$ colliders the photon couplings κ_A and λ_A can be probed besides of κ_G and λ_G at ep colliders. Due to accidental cancellations between the different contributions, \tilde{F}_j , for specific values of $\kappa_{A,G}, \lambda_{A,G}$ even smaller cross sections than that of the minimal vector coupling (M.C.) can be obtained. The cross section $\sigma_{M.C.}^{tot}$ for the case of HERA amounts to $0.2 pb$ only at the LEP bound⁸. For minimal vector coupling, the search limits at a rate of 10 events extend to 52 GeV ($|Q_\Phi| = 1/3$) and to 74 GeV ($|Q_\Phi| = 5/3$). Figure 3b shows the mass dependence of the integrated cross sections for vector leptoquark pair production at LEP \times LHC with $|Q_\Phi| = 1/3$. The search limits on a rate of 10 events for leptoquarks coupling to both photons and gluons with a minimal vector coupling extend from $M_\Phi = 185$ GeV to

⁷In [21] also limits on 1st and 2nd generation scalar leptoquarks are derived from a search in $e^+e^- \rightarrow \bar{S}S^* \leftrightarrow lq$ [22]. However, these bounds depend on assumptions made on λ_{lq} .

⁸Neither the LEP experiments nor searches at proton colliders have investigated vector leptoquarks so far allowing for general vector boson–gauge boson couplings (3). Since there is a symmetry in the decay pattern of scalar and vector leptoquarks (cf. [9], table 3), one finds from the cross sections calculated in [9] that the exclusion limit found for scalars at LEP holds for vectors as well.

270 GeV for $|Q_{\Phi}| = 1/3$ to $|Q_{\Phi}| = 5/3$ vector leptoquarks.

Note that the above bounds have been calculated on the basis of the direct contributions due to photon–gluon fusion only. The resolved photon contributions [10] will allow to extend the mass ranges correspondingly.

In summary we have shown that in a search for both scalar and vector leptoquark pair production at ep colliders yet open mass ranges can be explored independently of the size of the leptoquark–fermion couplings and fermion generation to which the leptoquarks are associated. For vector leptoquarks constraints on both the anomalous κ_A, λ_A and κ_G, λ_G can be derived.

Acknowledgement. We are grateful to Slava Ilyin and Sergey Shichanin for discussions. We would like to thank Günter Wolf and Peter Zerwas for conversations, and James Botts for reading the manuscript. E.B. would like to thank DESY–Zeuthen for the warm hospitality extended to him.

4 Appendix

The functions $F_i(\hat{s}, \beta, \cos \theta)$ of (12) are:

$$\begin{aligned}
F_0 &= 19 - 6\beta^2 + 6\beta^4 + (16 - 6\beta^2)\beta^2 \cos^2 \theta + 3\beta^4 \cos^4 \theta \\
F_1 &= -22 - 10\beta^2 \cos^2 \theta \\
F_2 &= 4 + \frac{\hat{s}}{M_{\Phi}^2} \frac{1 - \beta^4 \cos^4 \theta}{2} + \frac{\hat{s}^2}{M_{\Phi}^4} \frac{(1 - \beta^2 \cos^2 \theta)^2}{16} \\
F_3 &= 28 + 4\beta^2 \cos^2 \theta + \frac{\hat{s}}{M_{\Phi}^2} \beta^2 \cos^2 \theta (1 - \beta^2 \cos^2 \theta) + \frac{\hat{s}^2}{M_{\Phi}^4} \frac{(1 - \beta^2 \cos^2 \theta)^2}{8} \\
F_4 &= -5 + \beta^2 \cos^2 \theta + \frac{\hat{s}}{M_{\Phi}^2} \frac{-3 + \beta^2 \cos^2 \theta + 2\beta^4 \cos^4 \theta}{4} - \frac{\hat{s}^2}{M_{\Phi}^4} \frac{(1 - \beta^2 \cos^2 \theta)^2}{8} \\
F_5 &= \frac{3 - \beta^2 \cos^2 \theta}{4} + \frac{\hat{s}}{M_{\Phi}^2} \frac{5 - 4\beta^2 \cos^2 \theta - \beta^4 \cos^4 \theta}{16} \\
&+ \frac{\hat{s}^2}{M_{\Phi}^4} \frac{13 - 25\beta^2 \cos^2 \theta + 11\beta^4 \cos^4 \theta + \beta^6 \cos^6 \theta}{128} \\
F_6 &= -4 + 4\beta^2 \cos^2 \theta \\
F_7 &= 4 + \frac{\hat{s}}{M_{\Phi}^2} \frac{-7 + 8\beta^2 \cos^2 \theta - \beta^4 \cos^4 \theta}{2} + \frac{\hat{s}^2}{M_{\Phi}^4} \frac{(1 - \beta^2 \cos^2 \theta)^2}{2} \\
&+ \frac{\hat{s}^3}{M_{\Phi}^6} \frac{(1 - \beta^2 \cos^2 \theta)^3}{16} \\
F_8 &= -\frac{\hat{s}}{M_{\Phi}^2} (1 - \beta^2 \cos^2 \theta) + \frac{\hat{s}^2}{M_{\Phi}^4} \frac{11 - 13\beta^2 \cos^2 \theta + \beta^4 \cos^4 \theta + \beta^6 \cos^6 \theta}{8} \\
&- \frac{\hat{s}^2}{M_{\Phi}^4} \frac{(1 - \beta^2 \cos^2 \theta)^3}{8} \\
F_9 &= 1 - \beta^2 \cos^2 \theta + \frac{\hat{s}}{M_{\Phi}^2} \frac{-3 + 4\beta^2 \cos^2 \theta - \beta^4 \cos^4 \theta}{2} + \frac{\hat{s}^2}{M_{\Phi}^4} (1 - \beta^2 \cos^2 \theta)^2 \\
&+ \frac{\hat{s}^3}{M_{\Phi}^6} \frac{-3 + 7\beta^2 \cos^2 \theta - 5\beta^4 \cos^4 \theta + \beta^6 \cos^6 \theta}{16}
\end{aligned}$$

$$\begin{aligned}
F_{10} &= \frac{3 - \beta^2 \cos^2 \theta}{4} + \frac{\hat{s}}{M_{\Phi}^2} \frac{-19 + 20\beta^2 \cos^2 \theta - \beta^4 \cos^4 \theta}{16} \\
&+ \frac{\hat{s}^2}{M_{\Phi}^4} \frac{141 - 249\beta^2 \cos^2 \theta + 107\beta^4 \cos^4 \theta + \beta^6 \cos^6 \theta}{128} \\
&+ \frac{\hat{s}^3}{M_{\Phi}^6} \frac{-53 + 119\beta^2 \cos^2 \theta - 79\beta^4 \cos^4 \theta + 13\beta^6 \cos^6 \theta}{128} \\
&+ \frac{\hat{s}^4}{M_{\Phi}^8} \frac{27 - 68\beta^2 \cos^2 \theta + 58\beta^4 \cos^4 \theta - 20\beta^6 \cos^6 \theta + 3\beta^8 \cos^8 \theta}{512} \\
F_{11} &= -8 + \frac{\hat{s}}{M_{\Phi}^2} (3 - 4\beta^2 \cos^2 \theta + \beta^4 \cos^4 \theta) \\
F_{12} &= \frac{\hat{s}}{M_{\Phi}^2} (2 - 3\beta^2 \cos^2 \theta + 4\beta^4 \cos^4 \theta) \\
F_{13} &= -2(1 - \beta^2 \cos^2 \theta) + \frac{\hat{s}}{M_{\Phi}^2} \frac{9 - 13\beta^2 \cos^2 \theta + 4\beta^4 \cos^4 \theta}{4} \\
&- \frac{\hat{s}^2}{M_{\Phi}^4} \frac{2 - 3\beta^2 \cos^2 \theta + \beta^4 \cos^4 \theta}{2} + \frac{\hat{s}^3}{M_{\Phi}^6} \frac{(1 - \beta^2 \cos^2 \theta)^3}{16} \\
F_{14} &= -5 + \beta^2 \cos^2 \theta + \frac{\hat{s}}{M_{\Phi}^2} \frac{7 - 8\beta^2 \cos^2 \theta + \beta^4 \cos^4 \theta}{2} - 3 \frac{\hat{s}^2}{M_{\Phi}^4} \frac{(1 - \beta^2 \cos^2 \theta)^2}{8} \\
&- \frac{(1 - \beta^2 \cos^2 \theta)^3}{16} \\
F_{15} &= -\frac{3 - \beta^2 \cos^2 \theta}{2} + \frac{\hat{s}}{M_{\Phi}^2} \frac{13 - 14\beta^2 \cos^2 \theta + \beta^4 \cos^4 \theta}{8} \\
&- \frac{\hat{s}^2}{M_{\Phi}^4} \frac{41 - 81\beta^2 \cos^2 \theta + 39\beta^4 \cos^4 \theta + \beta^6 \cos^6 \theta}{64} \\
&+ \frac{\hat{s}^3}{M_{\Phi}^6} \frac{11 - 25\beta^2 \cos^2 \theta + 17\beta^4 \cos^4 \theta - 3\beta^6 \cos^6 \theta}{128} \\
F_{16} &= 1 - \beta^2 \cos^2 \theta - \frac{\hat{s}}{M_{\Phi}^2} \frac{3 - 5\beta^2 \cos^2 \theta + 2\beta^4 \cos^4 \theta}{4} \\
F_{17} &= \frac{3 - \beta^2 \cos^2 \theta}{4} - \frac{\hat{s}}{M_{\Phi}^2} \frac{7 - 8\beta^2 \cos^2 \theta + \beta^4 \cos^4 \theta}{16} \\
&- \frac{\hat{s}^2}{M_{\Phi}^4} \frac{3 - 7\beta^2 \cos^2 \theta + 5\beta^4 \cos^4 \theta - \beta^6 \cos^6 \theta}{128} + \frac{\hat{s}^3}{M_{\Phi}^6} \frac{(1 - \beta^2 \cos^2 \theta)^3}{32} \\
F_{18} &= 2(5 - \beta^2 \cos^2 \theta) - \frac{\hat{s}}{M_{\Phi}^2} \frac{11 - 15\beta^2 \cos^2 \theta + 4\beta^4 \cos^4 \theta}{4} \\
&- \frac{\hat{s}^2}{M_{\Phi}^4} \frac{(1 - \beta^2 \cos^2 \theta)^2}{4} \\
F_{19} &= 3 - \beta^2 \cos^2 \theta - \frac{\hat{s}}{M_{\Phi}^2} \frac{7 - 8\beta^2 \cos^2 \theta + \beta^4 \cos^4 \theta}{4} \\
&+ \frac{\hat{s}^2}{M_{\Phi}^4} \frac{11 - 13\beta^2 \cos^2 \theta + \beta^4 \cos^4 \theta + \beta^6 \cos^6 \theta}{32} \\
&+ \frac{\hat{s}^3}{M_{\Phi}^6} \frac{5 - 7\beta^2 \cos^2 \theta - \beta^4 \cos^4 \theta + 3\beta^6 \cos^6 \theta}{128}
\end{aligned}$$

$$\begin{aligned}
F_{20} &= -\frac{3 - \beta^2 \cos^2 \theta}{2} + \frac{\hat{s}}{M_{\Phi}^2} \frac{(1 - \beta^2 \cos^2 \theta)^2}{8} \\
&+ \frac{\hat{s}^2}{M_{\Phi}^4} \frac{11 - 23\beta^2 \cos^2 \theta + 13\beta^4 \cos^4 \theta - \beta^6 \cos^6 \theta}{64}
\end{aligned} \tag{17}$$

The functions $\tilde{F}_i(\hat{s}, \beta)$, which describe the different contributions to the integrated cross section (13), are:

$$\begin{aligned}
\tilde{F}_0 &= \beta \left(\frac{11}{2} - \frac{9}{4}\beta^2 + \frac{3}{4}\beta^4 \right) - \frac{3}{8} (1 - \beta^2 - \beta^4 + \beta^6) \ln \left| \frac{1 + \beta}{1 - \beta} \right| \\
\tilde{F}_1 &= -4\beta - \frac{3}{4} (1 - \beta^2) \log \left| \frac{1 + \beta}{1 - \beta} \right| \\
\tilde{F}_2 &= \frac{1}{16} \beta \frac{\hat{s}}{M_{\Phi}^2} + \frac{3 - \beta^2}{4} \log \left| \frac{1 + \beta}{1 - \beta} \right| \\
\tilde{F}_3 &= 3\beta + \frac{1}{8} \beta \frac{\hat{s}}{M_{\Phi}^2} + \left(2 - \frac{3}{2}\beta^2 \right) \log \left| \frac{1 + \beta}{1 - \beta} \right| \\
\tilde{F}_4 &= -\frac{1}{8} \beta \frac{\hat{s}}{M_{\Phi}^2} + \left(-1 + \frac{3}{8}\beta^2 \right) \log \left| \frac{1 + \beta}{1 - \beta} \right| \\
\tilde{F}_5 &= -\frac{1}{96} \beta + \frac{5}{48} \beta \frac{\hat{s}}{M_{\Phi}^2} + \frac{4 - \beta^2}{16} \log \left| \frac{1 + \beta}{1 - \beta} \right| \\
\tilde{F}_6 &= -\frac{1}{2} (1 - \beta^2) \log \left| \frac{1 + \beta}{1 - \beta} \right| \\
\tilde{F}_7 &= \frac{7}{12} \beta \frac{\hat{s}}{M_{\Phi}^2} + \frac{1}{24} \beta \frac{\hat{s}^2}{M_{\Phi}^4} - \frac{5 + \beta^2}{4} \log \left| \frac{1 + \beta}{1 - \beta} \right| \\
\tilde{F}_8 &= -\frac{1}{6} \beta + \frac{1}{4} \beta \frac{\hat{s}}{M_{\Phi}^2} - \frac{1}{12} \beta \frac{\hat{s}^2}{M_{\Phi}^4} + \left(-\frac{1}{2} + \frac{1}{2} \frac{\hat{s}}{M_{\Phi}^2} \right) \log \left| \frac{1 + \beta}{1 - \beta} \right| \\
\tilde{F}_9 &= -\frac{1}{2} \beta + \frac{11}{12} \beta \frac{\hat{s}}{M_{\Phi}^2} - \frac{1}{6} \beta \frac{\hat{s}^2}{M_{\Phi}^4} - \frac{3 + \beta^2}{8} \log \left| \frac{1 + \beta}{1 - \beta} \right| \\
\tilde{F}_{10} &= -\frac{1}{96} \beta + \frac{59}{80} \beta \frac{\hat{s}}{M_{\Phi}^2} - \frac{113}{320} \beta \frac{\hat{s}^2}{M_{\Phi}^4} + \frac{43}{960} \beta \frac{\hat{s}^3}{M_{\Phi}^6} + \left(-\frac{1}{2} - \frac{1}{16} \beta^2 + \frac{1}{8} \frac{\hat{s}}{M_{\Phi}^2} \right) \log \left| \frac{1 + \beta}{1 - \beta} \right| \\
\tilde{F}_{11} &= \frac{1}{2} (1 + \beta^2) \log \left| \frac{1 + \beta}{1 - \beta} \right| \\
\tilde{F}_{12} &= \beta + \frac{1}{2} \log \left| \frac{1 + \beta}{1 - \beta} \right| \\
\tilde{F}_{13} &= \beta - \frac{5}{12} \beta \frac{\hat{s}}{M_{\Phi}^2} + \frac{1}{24} \beta \frac{\hat{s}^2}{M_{\Phi}^4} + \left[-\frac{1}{4} \frac{\hat{s}}{M_{\Phi}^2} + \left(\frac{3}{8} + \frac{1}{4} \beta^2 \right) \right] \log \left| \frac{1 + \beta}{1 - \beta} \right| \\
\tilde{F}_{14} &= -\frac{11}{24} \beta \frac{\hat{s}}{M_{\Phi}^2} - \frac{1}{24} \beta \frac{\hat{s}^2}{M_{\Phi}^4} + \frac{9 + 3\beta^2}{8} \log \left| \frac{1 + \beta}{1 - \beta} \right| \\
\tilde{F}_{15} &= \frac{1}{48} \beta - \frac{59}{96} \beta \frac{\hat{s}}{M_{\Phi}^2} + \frac{5}{64} \beta \frac{\hat{s}^2}{M_{\Phi}^4} + \frac{5 + \beta^2}{8} \log \left| \frac{1 + \beta}{1 - \beta} \right| \\
\tilde{F}_{16} &= -\frac{1}{2} \beta - \frac{1}{8} \beta^2 \log \left| \frac{1 + \beta}{1 - \beta} \right|
\end{aligned}$$

$$\begin{aligned}
\tilde{F}_{17} &= -\frac{1}{96}\beta + \frac{1}{48}\beta\frac{\hat{s}}{M_{\Phi}^2} + \frac{1}{48}\beta\frac{\hat{s}^2}{M_{\Phi}^4} - \frac{2+\beta^2}{16}\log\left|\frac{1+\beta}{1-\beta}\right| \\
\tilde{F}_{18} &= -\frac{1}{4}\beta\frac{\hat{s}}{M_{\Phi}^2} - \frac{1-6\beta^2}{8}\log\left|\frac{1+\beta}{1-\beta}\right| \\
\tilde{F}_{19} &= -\frac{1}{24}\beta + \frac{7}{96}\beta\frac{\hat{s}}{M_{\Phi}^2} + \frac{3}{64}\beta\frac{\hat{s}^2}{M_{\Phi}^4} + \left[\frac{1}{8}\frac{\hat{s}}{M_{\Phi}^2} - \frac{2+\beta^2}{4}\right]\log\left|\frac{1+\beta}{1-\beta}\right| \\
\tilde{F}_{20} &= \frac{1}{48}\beta + \frac{1}{6}\beta\frac{\hat{s}}{M_{\Phi}^2} - \frac{1}{8}(1-\beta^2)\log\left|\frac{1+\beta}{1-\beta}\right|
\end{aligned} \tag{18}$$

References

- [1] J.C. Pati and A. Salam, Phys. Rev. **D10** (1974) 275;
E. Farhi and L. Susskind, Phys. Rep. **74** (1981) 277;
L. Lyons, Progr. Part. Nucl. Phys. **10** (1982) 227;
B. Schrempp and F. Schrempp, DESY 84–055 (1984); Phys. Lett. **B153** (1985) 101;
J.L. Hewett and T.G. Rizzo, Phys. Rep. **183** (1989) 193;
P.H. Frampton, Mod. Phys. Lett. **A7** (1992) 559.
- [2] J. Wudka, Phys. Lett. **B167** (1986) 337.
- [3] W. Buchmüller, R. Rückl, and D. Wyler, Phys. Lett. **B191** (1987) 442.
- [4] M. Derrick et al., ZEUS collaboration, Phys. Lett. **B306** (1993) 173;
I. Abt et al., H1 collaboration, Nucl. Phys. **B396** (1993) 3.
- [5] M. Leurer, Phys. Rev. Lett. **71** (1993) 1324; Phys. Rev. **D49** (1994) 333; WIS–93/119/Dec–PH.
- [6] S. Rudaz and J. Vermaseren, CERN TH 2961 (1980), and corrigendum.
- [7] see e.g.: A.I. Akhiezer and V.B. Berestetskii, Quantum Electrodynamics, (Interscience, New York, 1965), Ch. IX and references therein.
- [8] K. Gaemers and G. Gounaris, Z. Phys. **C1** (1979) 259;
K. Hagiwara, R. Peccei, D. Zeppenfeld, and K. Hikasa, Nucl. Phys. **B282** (1987) 253.
- [9] J. Blümlein and R. Rückl, Phys. Lett. **B304** (1993) 337.
- [10] J. Blümlein and E. Boos, in preparation.
- [11] S.Y. Choi and F. Schrempp, in: Proc. of the Workshop ‘ e^+e^- Collisions at 500 GeV: The Physics Potential’, DESY 92–123B, August 1992, et. P. Zerwas, p. 793. Note that a few misprints are contained in eq. (12) of Phys. Lett. **B272** (1991) 149.
- [12] S. Frixione, M. Mangano, P. Nason, and G. Ridolfi, Phys. Lett. **B319** (1993) 339.
- [13] S.K. Jones and C.H. Llewellyn–Smith, Nucl. Phys. **B217** (1983) 145;
R. Rückl in: ‘Fundamental Physics’, Proc of the 13th International Winter Meeting, Cuenca, Spain, April 1985, eds. M. Aguilar–Benitez and A. Ferrando, (Inst. Estud. Nucl., Madrid, 1986), (transparencies) p. 288;
A. Dobado, M.J. Herrero, and C. Muñoz, Phys. Lett. **B191** (1987) 449.

- [14] J. Blümlein, DESY 93–132, Proc. of the 2nd Workshop ‘Physics and Experiments with Linear e^+e^- Colliders’, Waikoloa, HI, April 26–30, 1993, eds. F.A. Harris, S. Olsen, S. Pakvasa, and X. Tata, (World Scientific, Singapore, 1993) Vol. **II**, p. 524;
 DESY 93–153, Proc. of the Workshop, ‘ e^+e^- Collisions at 500 GeV’, Munich–Annecy–Hamburg, 1993, ed. P. Zerwas, (DESY, Hamburg, 1993), p. 419;
 J. Blümlein and E. Boos, Proc. of the Workshop ‘Physics at LEP200 and Beyond’, Teupitz, Germany, April 11–15 1994, eds. T. Riemann and J. Blümlein, Nucl. Phys. **B** (Proc. Suppl.) (1994).
- [15] E. Boos et al., Proc of the XXVIth Rencontre de Moriond, ed. I. Tran Than Van, (Edition Frontiers, Paris, 1991), p. 501;
 E. Boos et al., Proc of the 2nd Int. Workshop on Software Engineering, ed. D. Perret–Gallix, (World Scientific, Singapore, 1992), p. 665;
 E. Boos et al., KEK–preprint 92–47, 1992.
- [16] G. Tupper and M.A. Samuel, Phys. Rev. **D23** (1981) 1933;
 S.A. Bludman and J.A. Young, Phys. Rev. **126** (1962) 303;
 A.P. Sathe, Phys. Rev. **D11** (1975) 1940;
 A.C.T. Wu, T.T. Wu, and K. Fuchel, Phys. Rev. Lett., **11** (1963) 390;
 S.M. Berman and Y.S. Tsai, Phys. Rev. Lett. **11** (1963) 483;
 V.G. Kompaniets, Sov. Journ. Nucl. Phys., **12** (1971) 447; Yad. Fiz. **12** (1970) 826;
 O.P. Sushkov, V.V. Flambaum, and I.B. Khriplovich, Sov. Journ. Nucl. Phys. **20** (1975) 537; Yad. Fiz. **20** (1974) 1016.
- [17] J.D. Bjorken and S.D. Drell, Relativistic Quantum Mechanics, (McGraw–Hill, New York, 1964), p. 290.
- [18] J. Botts, J. Morfin, J. Owens, J. Qiu, W. Tung, and H. Weerts, CTEQ collaboration, East Lansing preprint, MSU–HEP 93/18 (1993).
- [19] A.D. Martin, W. J. Stirling, and R.G. Roberts, Durham preprint DTP–93–86, Oct. 1993;
 M. Glück, E. Reya, and A. Vogt, Z. Phys. **C48** (1990) 401.
- [20] D. Alexander et al., OPAL Collaboration, Phys. Lett. **B275** (1992) 123;
 D. Decamp et al., ALEPH Collaboration, Phys. Rep. **216** (1992) 253;
 O. Adriani, L3 Collaboration, Phys. Rep. **236** (1993) 1.
- [21] P. Abreu et al., DELPHI collaboration, Phys. Lett. **B316** (1993) 620.
- [22] N. Tracas and S. Vlassopoulos, Phys. Lett. **B220** (1989) 285.
- [23] J. Alitti et al., UA2 Collaboration, Phys. Lett. **B274** (1992) 507.
- [24] F. Abe et al., CDF Collaboration, Phys. Rev. **D48** (1993) R3939;
 S. Abachi et al., D0 Collaboration, Phys. Rev. Lett. **72** (1994) 965.

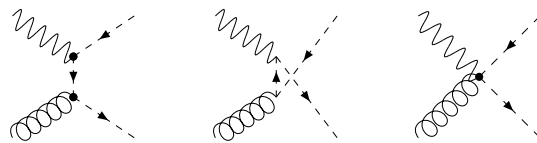


Figure 1: Diagrams describing leptoquark pair production via γ - g fusion

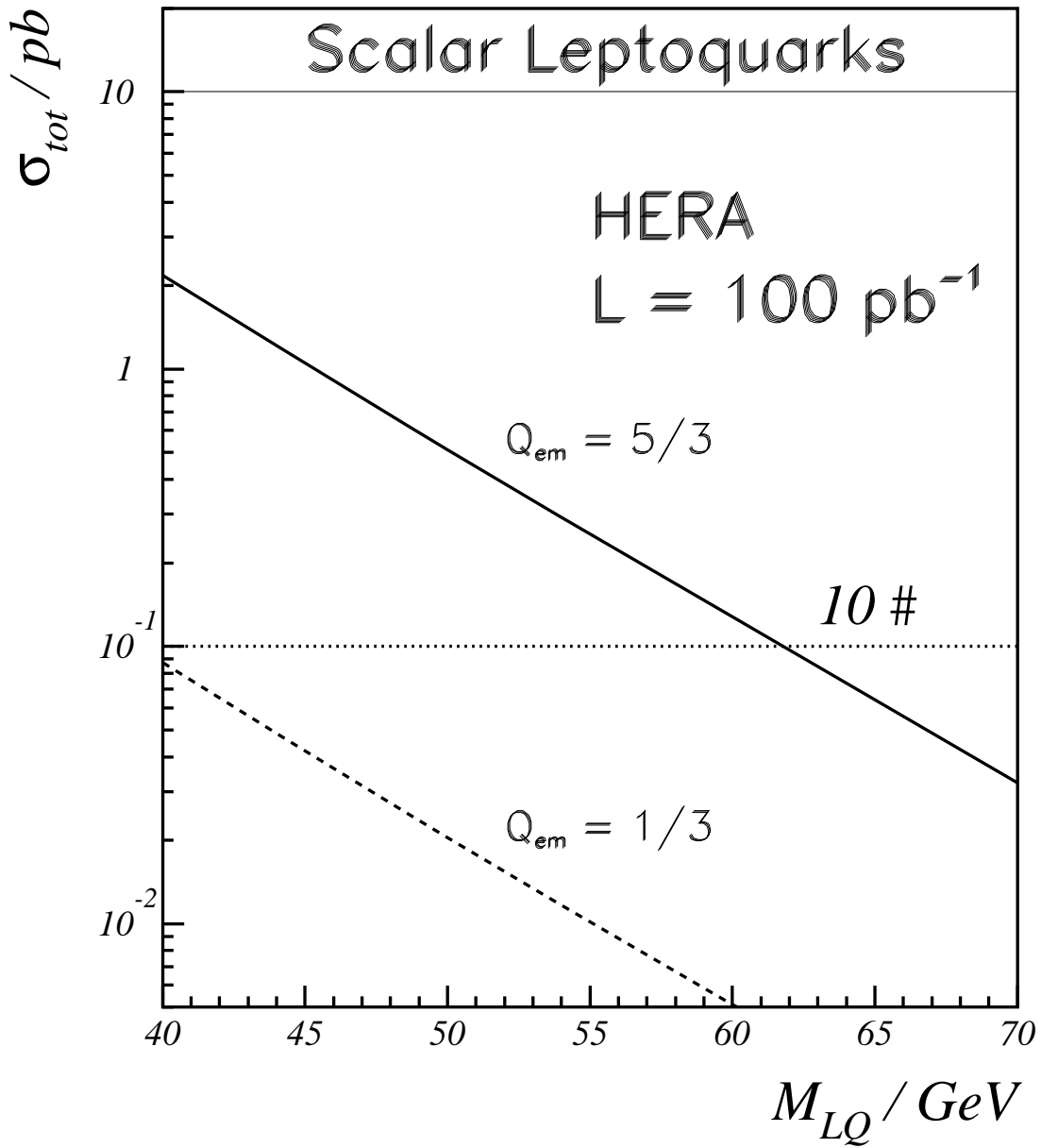


Figure 2a: Integrated cross sections for scalar leptoquark pair production, $\sqrt{s} = 314 \text{ GeV}$.

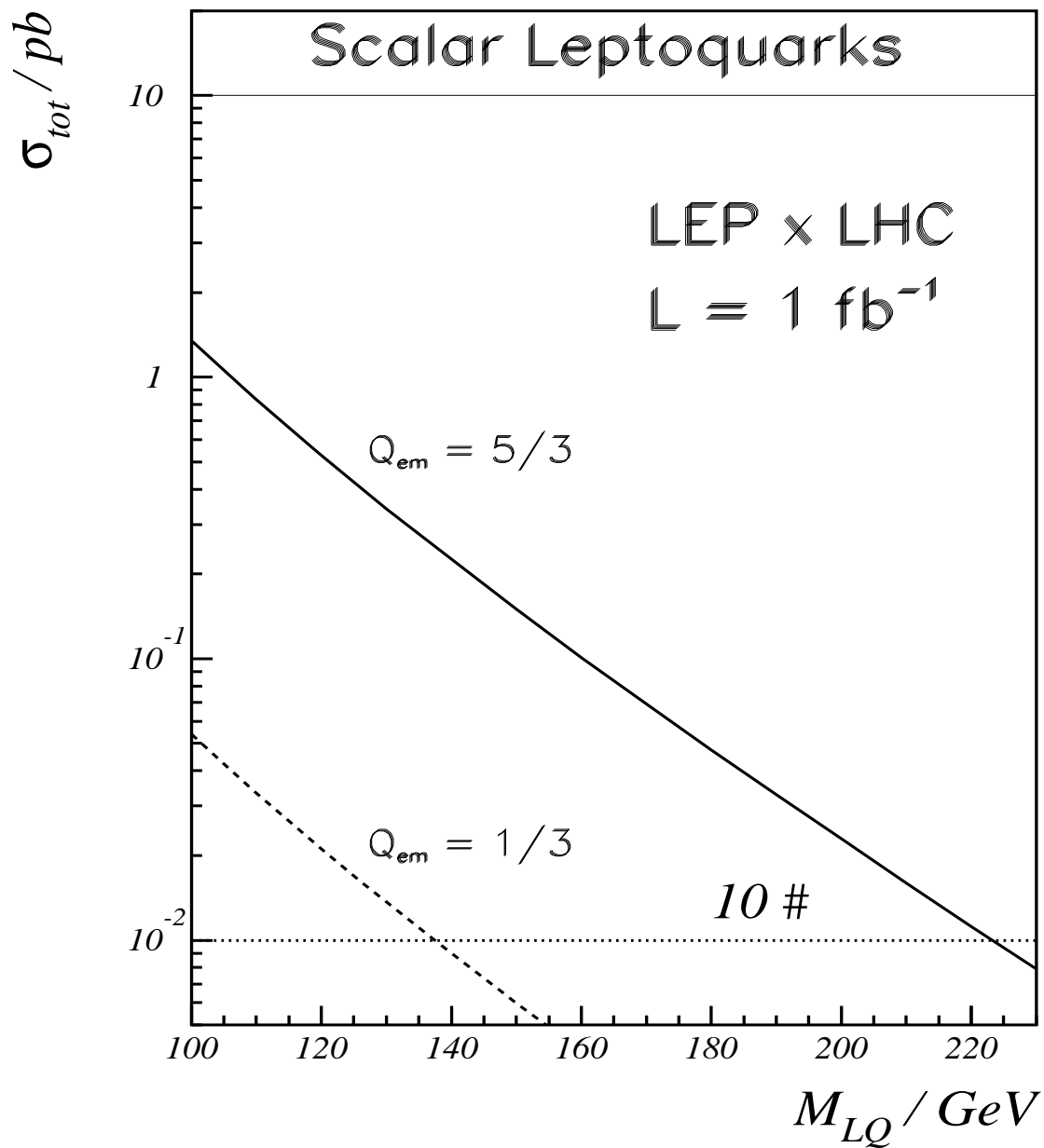


Figure 2b: Integrated cross sections for scalar leptoquark pair production, $\sqrt{s} = 1260$ GeV.

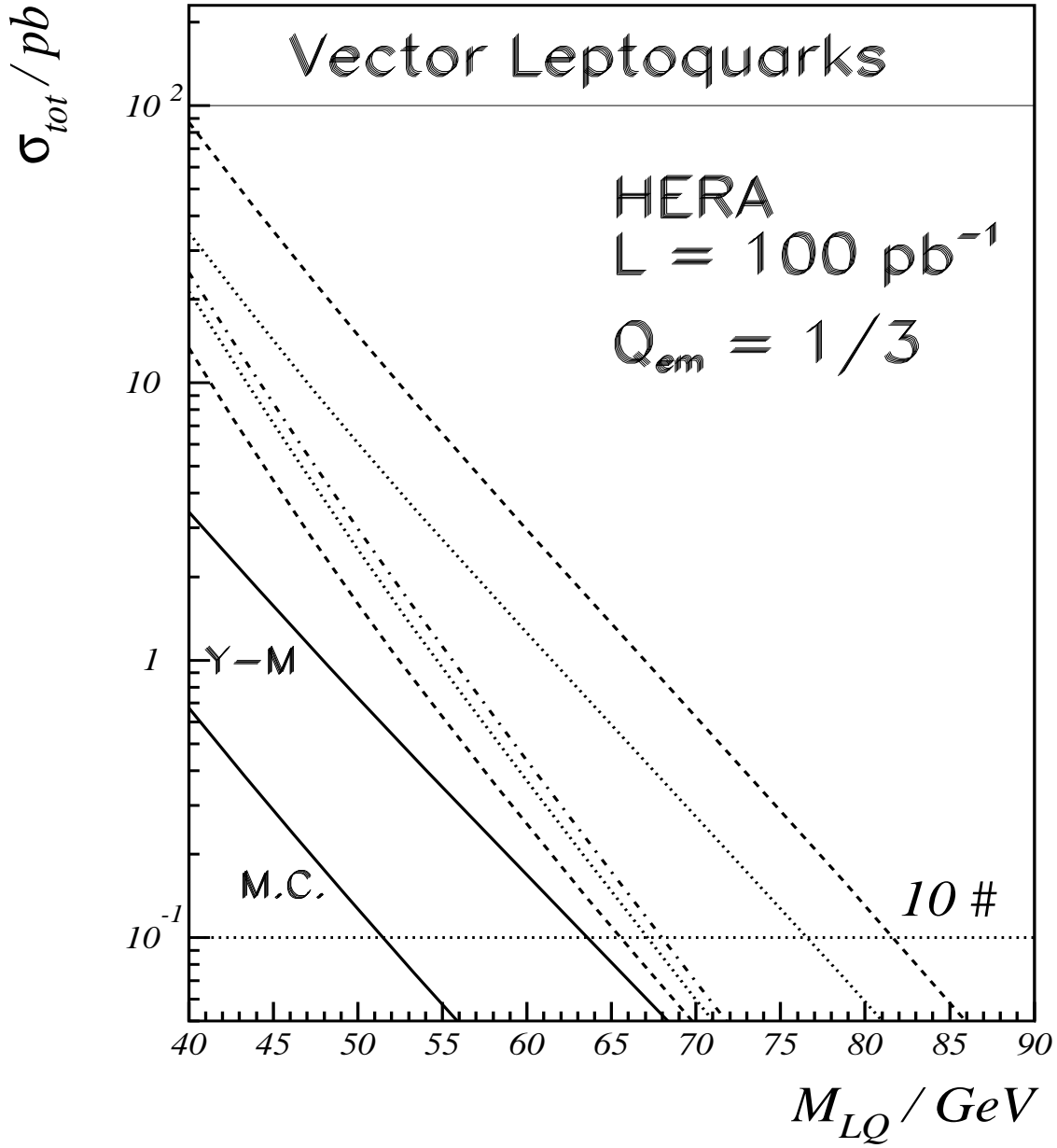


Figure 3a: Integrated cross sections for vector leptoquark pair production for $\sqrt{S} = 314 \text{ GeV}$ and different values of $\kappa_{A,G}$ and $\lambda_{A,G}$. Full lines: minimal coupling (M.C.) $\kappa_{A,G} = 1, \lambda_{A,G} = 0$, and Yang-Mills coupling (Y-M) $\kappa_{A,G} = \lambda_{A,G} = 0$. Upper dashed line: $\kappa_{A,G} = \lambda_{A,G} = -1$, lower dashed line: $\kappa_{A,G} = \lambda_{A,G} = 1$; upper dotted line: $\kappa_{A,G} = -1, \lambda_{A,G} = 1$; lower dotted line: $\kappa_{A,G} = 1, \lambda_{A,G} = -1$; dash-dotted line: $\kappa_A = 1, \kappa_G = -1, \lambda_A = 1, \lambda_G = -1$.

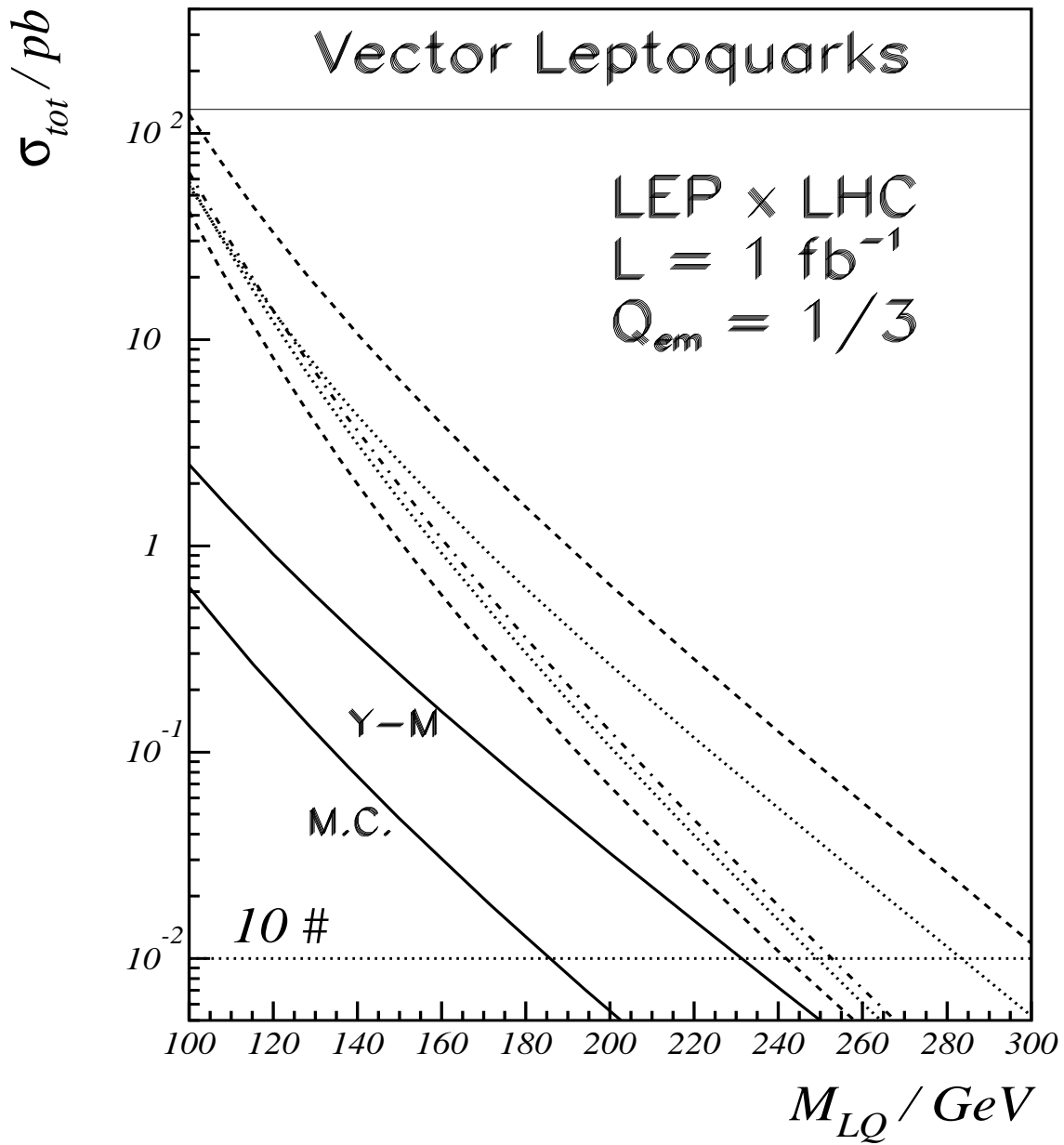


Figure 3b: Integrated cross sections for vector leptoquark pair production for $\sqrt{S} = 1260 \text{ GeV}$. The other parameters are the same as in figure 3a.